Bubble distributions and dynamics: The expansion-coalescence equation

S. Lovejoy
Department of Physics, McGill University, Montréal, Quebec, Canada

H. Gaonac'h
Centre for Research in Geochemistry and Geodynamics, Université du Québec à Montréal, Montréal, Quebec, Canada

D. Schertzer
Centre d'Enseignement et de Recherche sur l'Eau, Ecole Nationale des Ponts et Chaussées, Marne-la-Vallée, France

Received 2 October 2003; revised 2 April 2004; accepted 8 June 2004; published 13 November 2004.

[1] As magma rises from depth, it forms bubbles by nucleation, followed by diffusion-decompressive expansion. Expansion induces shearing, and shearing in turn causes coalescence. As the bubbles grow larger, coalescence gradually becomes more efficient and can be dominant. Coalescence first as a binary (bubble-bubble) and later as a (possibly singular percolating) multibody process may thus be central to eruption dynamics. Here we consider a binary coalescence model governed by the Smoluchowski or coalescence/coagulation equation. The introduction of decompressive expansion is theoretically straightforward and yields the nonlinear partial integrodifferential expansion-coalescence equation; we argue that this is a good model for bubble-bubble dynamics in a decompressing magma. We show that when the collision/interaction kernel has the same form over a wide range of interaction volumes (i.e., it is scaling), exact truncated power law solutions are possible irrespective of the expansion and the collision rate histories. This enables us to reduce the problem to a readily solvable linear ordinary differential equation whose solutions primarily depend on the total interaction integral. In this framework, we investigate the behavior of several eruption models. The validity of the expansion coalescence model is empirically supported by analysis of samples of pumice and lava. Theoretically, the suggested power laws are indeed stable and attractive under a wide range of conditions. We finally point out the effect of small perturbations and new ways to test the theory. *INDEX TERMS:* 8414 Volcanology: Eruption mechanisms; 8439 Volcanology: Physics and chemistry of magma bodies; 3220 Mathematical Geophysics: Nonlinear dynamics; 3210 Mathematical Geophysics: Modeling; *KEYWORDS:* expansion-coalescence, bubbles, fragmentation

Citation: Lovejoy, S., H. Gaonac'h, and D. Schertzer (2004), Bubble distributions and dynamics: The expansion-coalescence equation, *J. Geophys. Res.*, *109*, B11203, doi:10.1029/2003JB002823.

1. Introduction

1.1. Role of Coalescence in Volcano Dynamics

[2] Volcanic bubble growth is a fundamental but not yet fully understood part of both eruptive and effusive volcano dynamics. The basic picture starts at depth (see Figure 1) where the magma rises until nucleation starts. This occurs, depending on the amount of gas initially dissolved in the magma and on whether the latter is heterogeneous or homogeneous [*Mangan and Sisson*, 2000], somewhere between 200 and 60 MPa. This is followed by diffusion and decompressive expansion. However, the rate of coalescence-expansion will increase with the vesicularity of the ascending magma; it can, at least in principle, eventually become the dominant mechanism [*Gaonac'h et al.*, 1996b]. Somewhere around 10 MPa the vesicularity reaches a critical value of ~70% (e.g., *Sparks* [1978] gives 75% and *Gardner et al.* [1996] gives 64%), the magma fragments, and, if it is highly stressed, explosion occurs.

[3] Recently, there has been a growing consensus about the importance of coalescence growth processes, at least for large bubbles at high vesicularities. First, there is direct evidence for this in dynamical laboratory experiments [*Manga and Stone*, 1994]. There is also evidence for this in natural samples; sections of volcanic products including those from viscous magmas [e.g., *Gaonac'h et al.*, 2004] frequently display morphologies highly suggestive of bubble shear and coalescence (see, e.g., Figure 2a). Numerous empirical attempts to "decoalesce" bubbles before estimating their size distributions are based on this conviction. Perhaps the most compelling argument for the

0148-0227/04/2003JB002823$09.00

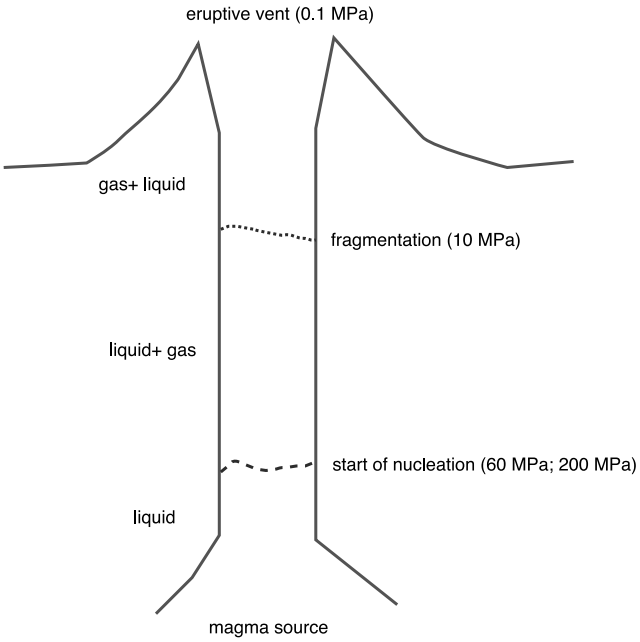

Figure 1. A schematic diagram showing the basic picture for an explosive eruption. See color version of this figure in the HTML.

central role of coalescence is the growing recognition that empirical bubble distributions follow power laws; that is, that the number density is of the form $\boldsymbol{n}(\boldsymbol{V}) \approx \boldsymbol{V}^{-B-1}$, where $\boldsymbol{V}$ is the bubble volume and B is a scaling exponent [e.g., *Gaonac'h et al.*, 1996a, 2004; *Simakin et al.*, 1999; *Blower et al.*, 2001; *Klug et al.*, 2002] (Figure 2b).

[4] Although with appropriate extra constraints/boundary conditions, it is theoretically possible to obtain power law distributions with pure nucleation-diffusion processes (e.g., *Blower et al.* [2001] for a four bubble hierarchical packing model) not only does coalescence provide a simple and natural intrinsic mechanism but, as emphasized by *Gaonac'h et al.* [1996b, 2004], binary coalescence immediately provides a unifying explanation for the apparent empirical universality of the exponent $B \approx 0.85$ in diverse volcanic products. Finally, using Monte Carlo simulations, *Gaonac'h et al.* [2003] have quantitatively shown how such power laws allow bubbles to be very efficiently "packed", effectively delaying the onset of "percolation" until vesicularities of the order of 0.70 are reached. At the percolation point, bubbles overlap to such a degree that there is almost surely a single large (tentacle-like) bubble spanning an infinite system: the magma is effectively reduced to fragments by the network of overlapping bubbles. If it is stressed, this triggers an explosion. Note that this is very different from the usually postulated eruption mechanisms in which fragmentation is the consequence, not the cause, of either the stress or the strain rates exceeding critical thresholds. Here we are referring to power law (algebraic) number-size distributions; this should not be confused with the totally different single bubble growth rate which may also be a power law (see Appendix A).

[5] Finally, we should mention that while our results may help explain some of the early stages in the evolution of foams, they are not expected to be relevant to the evolution of foams per se. This is because bubble interactions in foams are multibubble, not just binary. The picture that emerges from this is one in which coalescence, both binary at lower vesicularities and multibody near the percolation point, plays a central role (see Figure 3 for a schematic). As before, it starts with a rising magma with nucleation, diffusion, decompressive expansion. However, diffusion and other single bubble processes are linear in the number density where as binary coalescence is quadratic. Eventually, vesicularities can be high enough so that binary coalescence becomes dominant over single bubble processes; the coales-

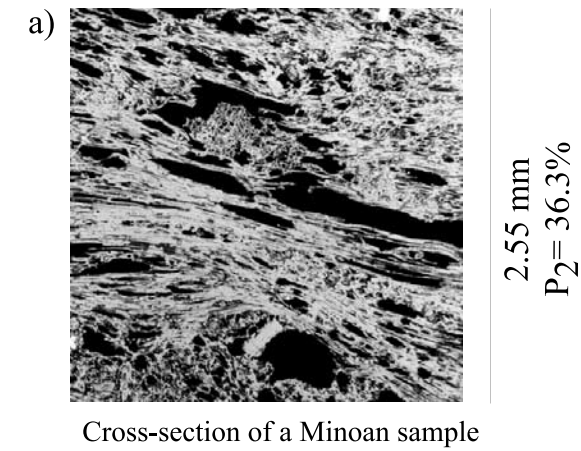

Figure 2. (a) Digitization of a Minoan pumice sample from Santorini, more details on the eruption are given by *Gardner et al.* [1996]. (b) Plots of the number of vesicles from the digitized surface of a single Minoan eruption volcanic sample of size larger and smaller than $\boldsymbol{A}$ ($\boldsymbol{A}$ in mm^2), $\mathbf{N}_2(\boldsymbol{A}' > \boldsymbol{A})$, $\mathbf{N}_2(\boldsymbol{A}' < \boldsymbol{A})$ versus $\boldsymbol{A}$ for sample in Figure 2a (these are integrals of $\boldsymbol{n}(\boldsymbol{A})$). The subscripts indicate the dimension of space, 2 for cross sections. A line with slope $B_2 = 0.75$ is shown ($B_2 = -$slope, the subscript indicates the dimension of space of the sampling, for $\mathbf{N}_2(\boldsymbol{A}' < \boldsymbol{A})$ the corresponding exponent for small bubbles is -0.20). The corresponding volume exponents are $B = B_3 = 0.85$ (large bubbles) and +0.20 (small bubbles). To change dimension from 2 to 3, we use $B_3 = 2B_2/3 + 1/3$ (which is strictly valid only for convex bubbles [*Gaonac'h et al.*, 1996a]).

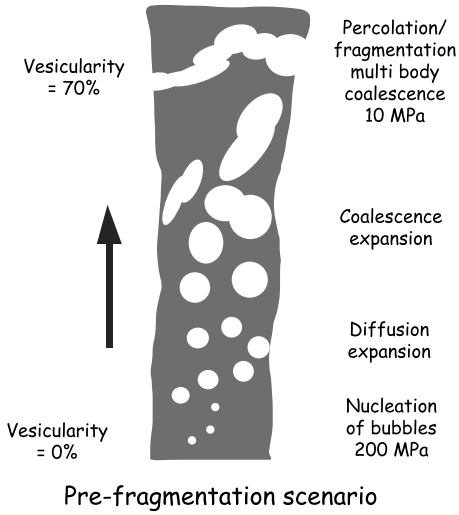

Figure 3. A schematic of the emerging picture showing the central role of coalescence. See color version of this figure in the HTML.

cence power law regime is established (the exact theoretical criterion for dominance is given by *Gaonac'h et al.* [1996b]). As the vesicularity increases further, the rates of ternary and higher-order collisions become dominant diverging at a critical vesicularity P_c: at this point, the entire magma fragments [*Gaonac'h et al.*, 2003]. In stressed magmas the fragmentation signals explosion; the process is suddenly quenched; the resulting samples display the entire range of bubbles. In effusive basalts the gas is nearly completely exsolved, equilibrium with atmospheric pressure is achieved, and the coalescence process has time to coalesce all the small bubbles while simultaneously decreasing the overall number density.

1.2. Modeling of Coalescence and the Coalescence Equation

[6] The understanding of bubble growth processes has mostly progressed in the areas of nucleation and diffusion, which are single bubble processes and are hence linear with respect to the bubble number density. They are relatively tractable mathematically and have been studied in laboratory experiments [e.g., *Simakin et al.*, 1999]. In contrast, coalescence is a binary (or higher-order) process and is hence nonlinear, accelerating notably as the vesicularity increases. Unfortunately, theoretical consideration of general coalescence processes would be intractable without a further guiding physical principle. Indeed, in spite of its potential importance, the coalescence equation has only occasionally been invoked in this context [*Sahagian*, 1985; *Gaonac'h et al.*, 1996b].

[7] In discussing effusive eruptions, it was argued [*Gaonac'h et al.*, 1996b] that until the vesicularity was very high, coalescence was primarily (but not necessarily exclusively) a binary bubble interaction. This simplification allowed the (binary) coalescence equation to be invoked, enabling the estimation of the relative rates of formation of bubbles of different sizes. Application of the binary coalescence equation showed that excluding decompression/expansion which affects all bubbles by an equal factor, for large bubbles coalescence can quickly become the dominant process, at least if there is a high enough bubble collision rate. The second application of the coalescence equation was to argue that, when the coalescence mechanism was particularly efficient for bubbles of roughly the same size, the process would have a cascade-like phenomenology. Beyond that, the cascade model was not derivable from the coalescence equation; indeed, *Gaonac'h et al.* [1996b] proposed a quasi-steady state cascade process in which the volume scaling exponent B was determined by conservation of volume; hence it had to be near the value 1. Its deviation from unity could not be determined by the model.

1.3. A New Framework for Handling Coalescence: Coalescence-Expansion Equation

[8] The problem of binary collisions with the possibility of "sticking" is important in many areas of science. The mathematical formulation of the basic problem goes back to *Smoluchowski* [1916]; the resulting equation has been variously called the "Smoluchowski equation", "the coalescence equation", and the "coagulation equation" (see *Drake* [1972] for an early review). Today, major application areas include notably aerosol formation [see *Friedlander*, 1961; *Turco and Yu*, 1999], hydrometeor growth [e.g., *Srivastava and Passarelli*, 1980; *Brown*, 1995], polymer growth [*Lushnikov*, 1972; *Van Dongen*, 1987], nuclear reactions [e.g., *Meunier and Peschanski*, 1992], and astrophysics (especially planetary growth [e.g., *Lee*, 2000]). Although this is a nonlinear partial integrodifferential equation, a great deal is now known about long-time solutions, especially in the case where the fundamental interaction is "scaling" (i.e., when it depends only on ratios of particle sizes, the basic mechanism is scale-invariant). Of particular importance is the work by *Van Dongen and Ernst* [1987, 1988] and *Van Dongen* [1987], who provided a fairly complete classification of interaction "kernels" (see the function $\boldsymbol{H}$ in equation (1) below) as well as corresponding large time and large particle behaviors.

[9] When the volcanic bubble collision/collection kernel is scaling (sometimes also called "homogenous", see below) these power law solutions are stable and attractive. If the homogeneity exponent is β (see section 2), then the stable solutions are power laws with exponents $B = \beta$ and we can now turn the argument around and conclude that the observation of a distribution with a given B must have been the result of coalescence with a homogeneous kernel with scaling exponent β. The overall picture is thus of a dynamically evolving (still possibly cascade-like, but not quasi-steady state) cutoff power law distribution with an exponent fundamentally determined by the exponent of the bubble collision/collection kernel. Since pure coalescence doesn't alter the vesicularity (the total volume of the coalescing bubbles is conserved in a pure coalescence process), we must take into account expansion in order to obtain a realistic overall picture of the bubble size distribution.

[10] Before continuing, we need a few words on the structure of this paper. The writing has been a difficult task since the main result, the existence of stable, attractive truncated power law number distributions, is easy enough to state, but its derivation is nevertheless technically complex. We have attempted to put as many of the technical derivations as possible in appendices where readers may consult them. For readers primarily interested in results, the key sections are

section 2 where we introduce the notation and explain the assumptions, and section 3.4 where we give the basic truncated power law solutions. The rest of the paper consists of mathematical developments (sections 3.1 and 3.2), consequences (section 3.3), summary of key results (section 3.4), consequences for large bubbles (section 3.5), empirical tests (section 3.6), and conclusions (section 4). Appendices A and C on single bubble processes and examples, respectively, are intended to be primarily pedagogical, whereas Appendix B is concerned with a technically difficult linear stability calculation which, while fundamentally important in justifying the use of the equation in physical modeling, does not directly impinge on the rest of the development.

2. Expansion-Coalescence Equation

2.1. Mathematical Formulation of the Problem

[11] We first introduce the notation and equations; we then nondimensionalize them. The dimensional quantities will be written in bold, the nondimensional in plain (the only exception will be the time variable t; τ will be the nondimensional time); see Table 1 for a summary and definitions. Let the number density $\boldsymbol{n}(\boldsymbol{V}, t)$ equal the number of bubbles with volumes between $\boldsymbol{V}$ and $\boldsymbol{V} + \boldsymbol{dV}$ per unit volume (of space), $\boldsymbol{\xi}(t)$ be the rate of decompressive expansion (from any source) and let $\boldsymbol{\varphi}(t)$ be the coalescence rate (the total change in bubble volume per unit time due to coalescence). The expansion-coalescence equation can thus be written

$$\frac{\partial \boldsymbol{n}(\boldsymbol{V},t)}{\partial t} = -\boldsymbol{\xi}(t)\frac{\partial(\boldsymbol{V}\boldsymbol{n}(\boldsymbol{V},t))}{\partial \boldsymbol{V}} + \boldsymbol{\varphi}(t) \cdot \left[\begin{array}{l} \frac{1}{2}\int_0^{\boldsymbol{V}} \boldsymbol{H}(\boldsymbol{V}-\boldsymbol{V}',\boldsymbol{V}')\boldsymbol{n}(\boldsymbol{V}-\boldsymbol{V}',t)\boldsymbol{n}(\boldsymbol{V}',t)d\boldsymbol{V}' \\ -\boldsymbol{n}(\boldsymbol{V},t)\int_0^{\infty} \boldsymbol{H}(\boldsymbol{V},\boldsymbol{V}')\boldsymbol{n}(\boldsymbol{V}',t)d\boldsymbol{V}' \end{array} \right] \quad (1)$$

where $\boldsymbol{V}'$ is a dummy variable. The first term on the right-hand side represents the decompressive expansion of the bubble (see Appendix A for a detailed derivation), while the second term is due to coalescence; putting $\xi(t) = 0$ yields the standard (pure) coalescence equation. Although this notation for the coalescence processes may seem heavy, it is standard; in Appendix B we use a simpler though less conventional form. $\boldsymbol{H}(\boldsymbol{V}, \boldsymbol{V}')$ is the fraction of the overall coalescence per unit time which occurs between bubbles with volumes in the range $\boldsymbol{V}$ to $\boldsymbol{V} + \boldsymbol{dV}$ and the range $\boldsymbol{V}'$ to $\boldsymbol{V}' + \boldsymbol{dV}'$; it is the basic collision/collection "kernel". This interaction kernel describes the intensity of the interaction of two quantities that are integrated. Note that we do not consider the slightly more general case $\boldsymbol{H}(\boldsymbol{V}, \boldsymbol{V}', t)$ (i.e., the coalescence rate due to bubbles with volumes in the range $\boldsymbol{V}$ to $\boldsymbol{V} + \boldsymbol{dV}$ and the range $\boldsymbol{V}'$ to $\boldsymbol{V}' + \boldsymbol{dV}'$), where the factorization $\boldsymbol{H}(\boldsymbol{V}, \boldsymbol{V}', t) = \boldsymbol{\varphi}(t)\boldsymbol{H}(\boldsymbol{V}, \boldsymbol{V}')$ is impossible. Such a factorization of the time dependence of the coalescence process is justified when the bubble-bubble interaction mechanism ($\boldsymbol{H}$) is fixed; only the coalescence rate $\boldsymbol{\varphi}(t)$ changes in time (reflecting changes in viscosity, strain rates). The dimensions of $\boldsymbol{\varphi}(t)$ are chosen to be volume/time, this simplifies the nondimensionalization of $\boldsymbol{H}$; in the context of precise models of the interaction, it can be given a physical interpretation (below). Considering now the coalescence term, the first integral gives the time rate of change of bubble number density for volume $\boldsymbol{V}$ bubbles due to coalescence of smaller bubbles; the second integral accounts for the loss of bubbles of size $\boldsymbol{V}$ due to coalescence with either larger or smaller bubbles.

[12] Finally, the first term on the right of equation (1) represents a single bubble process term, the expansion of bubbles at rate $\boldsymbol{\xi}(t)$:$(d\boldsymbol{V}/dt) = \boldsymbol{\xi}(t)\boldsymbol{V}$; $\boldsymbol{\xi} > 0$ corresponds to expansion, $\boldsymbol{\xi} < 0$ corresponds to contraction. If we add the term $-\boldsymbol{\mu}(t)[\partial(\boldsymbol{n}\boldsymbol{V}^{1/3})/\partial \boldsymbol{V}]$, where $\boldsymbol{\mu}(t)$ is the diffusion rate of the dissolved gas into bubbles (dimensions area per unit time), then equation (1) is an expansion-diffusion-coalescence equation: see Appendix A for more information for this and other single bubble processes and terms. In what follows, we assume that the coalescence and expansion terms are dominant. In Appendix B we show how to treat other single bubble processes as small perturbations. Our results will only depend on certain symmetries of the kernel $\boldsymbol{H}$, and one convergence property; these are discussed below.

2.2. Nondimensional Expansion-Coalescence Equation

[13] The expansion-coalescence equation involves both dimensions of time and volume. Nondimensionalizing the volume can simply be accomplished by using the mean initial bubble volume $\boldsymbol{V}_0$ (the exact numerical value is unimportant):

$$V = \boldsymbol{V}/\boldsymbol{V}_0 \qquad n = \boldsymbol{V}_0^2\boldsymbol{n} \quad (2)$$

(note that the dimensions of $\boldsymbol{n}$ are volume^{-2} since $\boldsymbol{n}$ is the number density per unit interval of bubble volume $\boldsymbol{dV}$). Similarly, we have $\boldsymbol{H}(\boldsymbol{V}, \boldsymbol{V}') = \boldsymbol{H}(\boldsymbol{V}, \boldsymbol{V}')$ is dimensionless. We also have for the nondimensional expansion rate

$$\xi = \frac{\boldsymbol{\xi}}{\boldsymbol{\varphi}}\boldsymbol{V_0} \quad (3a)$$

Time can be nondimensionalized either by using the expansion rate $\boldsymbol{\xi}$ or the coalesence rate $\boldsymbol{\varphi}$. It turns out to be more convenient to use $\boldsymbol{\varphi}$:

$$\tau(t) = \boldsymbol{V}_0^{-1}\int_0^t \boldsymbol{\varphi}(t')dt' \quad (3b)$$

(assuming the process starts at $t = 0$). These definitions permit us to write the following nondimensional expansion-coalescence equation

$$\frac{\partial n}{\partial \tau} = -\xi(\tau)\frac{\partial(Vn)}{\partial V} + \frac{1}{2}\int_0^V H(V-V',V')n(V-V',\tau) \cdot n(V',\tau)dV' - n(V,\tau)\int_0^{\infty} H(V,V')n(V',\tau)dV' \quad (4)$$

2.3. Scaling Symmetries of Interaction Kernel

2.3.1. Scaling Symmetry ("Homogeneous") Kernel

[14] The scaling symmetry is the basic assumption. Physically, it is justified if over a range of volumes, the coalescence mechanism involves no characteristic volume. More precisely, this means that if the volumes of the interacting bubbles are increased by a factor λ that the interaction (the kernel H) increases by a power of λ;

Table 1. Symbols Used in the Text and Their Definitions[a]

Symbol	Meaning
V	bubble volume
V_0	characteristic bubble volume used for nondimensionalizing the volumes (e.g., the initial mean volume)
$V^*(t)$	truncation/cutoff bubble volume, roughly, the largest in the system
z	$V/V^*(t)$
$f(z)$	cutoff function specifying the exact form of the large V truncation
$g(z)$	subexponential part of f : $g(z) = f(z)e^z$
t	time
τ	nondimensional time
$n(V, t)$	number density of bubbles between V and $V + dV$
$n_0(t)$	time varying amplitude of the power law number density
N	number distribution; the integral of n from small to large ($N(\mathbf{V}' > \mathbf{V})$ or large to small $N(\mathbf{V}' < \mathbf{V})$). Subscripts indicate the dimension of space
$H(V, V')$	time-independent interaction kernel describing the interaction between bubbles of size V and V'
β	basic scaling exponent for H
ω	scaling exponent for the extreme V falloff H
$h_{0,0}$	fundamental interaction coefficient
$h_{q,q'}$	generalized interaction coefficient
$\xi(t)$	expansion rate as a function of time
$\varphi(t)$	coalescence rate (the total volume of bubbles per unit volume of space created by coalescence per unit time)
$\mu(t)$	diffusion rate as a function of time
$E(V, V')$	dimensionless efficiency factor for collisions between bubbles size V, V'
λ	scale ratio
$\Delta u(V, V')$	absolute velocity difference (shear) between bubbles volume V, V'
$u_0(\tau)$	velocity of bubbles with the reference volume V_0 (models with buoyancy generated shearing)
γ	velocity exponent with respect to volume (models with buoyancy generated shearing)
$P(t)$	vesicularity, the fraction of the volume occupied by bubbles
P_0	initial porosity of the system (when coalescence begins to act), equal to $P(0)$
F	total expansion (decompression) factor since the beginning of the coalescence process, equal to $P(t)/P(0)$
p_B	numerical factor of order unity relating the porosity and cutoff V^*
Γ	standard gamma function
G	ratio by which the largest bubbles increase in size purely due to coalescence processes
$w(V, t)$	rate of growth of a bubble of size V
δ	exponent of w with respect to V
H	interaction operator (Appendix B only)
$a(V, t)$	an arbitrary number density (Appendix B only)
$b(V, t)$	an arbitrary number density (Appendix B only)
N	V^{1+B} "compensated" number density (Appendix B only)
$\mathsf{N}\prime$	perturbation of $\mathsf{N}(Appendix B only)$
$\overline{\mathsf{N}'}(q, t)$	Mellin transform of N' (Appendix B only)
w_q	relative perturbation in the Mellin transform of number density (Appendix B only)
α	an exponent in a model eruption characterizing an eruption
τ_0	a parameter indicating the (dimensionless) time of eruption

[a]Symbols are in the approximate order in which they are introduced. In addition, we have used the convention that bold symbols are for dimensional quantities, and standard symbols are for their dimensionless counterparts. The only exception is t (dimensional time) and τ (dimensionless time).

the form of H is therefore independent of the scale, it is scale-invariant.

[15] Mathematically, for any bubble volume ratio λ:

$$H(\lambda V, \lambda V') = \lambda^{\beta} H(V, V') \tag{5a}$$

where β is the scaling/homogeneity exponent.

[16] Although virtually all interaction kernels studied in the literature are scaling/homogeneous, the justification here is both theoretical and empirical. First, a scaling form is appropriate when there is no qualitative change in the coalescence mechanism over wide ranges of bubble volume; such scaling (power law, with scale-invariant exponent) mechanisms are frequently obtained in fluid systems. Second, the scaling form can be justified ex post facto if the number densities do indeed display scaling (power law) regimes (as they appear to do here).

2.3.2. Exchange Symmetry

[17] If we also assume that the collisions are binary and that the mechanism depends only on the volumes, then we obtain an "exchange" symmetry:

$$H(V, V') = H(V', V) \tag{5b}$$

Note that virtually all the kernels that have been studied in the literature satisfy both the scaling and the exchange symmetries 1 and 2, these properties are very general.

[18] Combining equation (5a) and (5b) and using $\lambda = V'/V$, we deduce

$$V^{\beta} H(1, \lambda) = V^{\beta} H(\lambda, 1) = H(V, V') = H(V', V) \tag{6a}$$

$$H\left(1, \lambda^{-1}\right) = H\left(\lambda^{-1}, 1\right) = \lambda^{-\beta} H(\lambda, 1) = \lambda^{-\beta} H(1, \lambda) \tag{6b}$$

2.3.3. Convergence of the Nondimensional Interaction Coefficient $h_{0,0}$

[19] The final property that we need is a bit technical; it has to do with the convergence (finiteness) of various coalescence integrals. Define the dimensionless "interaction coefficient" between bubbles $h_{0,0}$ as

$$h_{0,0} = \int_0^{\infty} \left[1 - \frac{1}{2}(1+\lambda)^{\beta}\right] \lambda^{-1-\beta} H(1, \lambda) d\lambda$$

$$= \int_1^{\infty} \left[1 + \lambda^{\beta} - (1+\lambda)^{\beta}\right] \lambda^{-1-\beta} H(1, \lambda) d\lambda \tag{7}$$

The equality of the two integrals follows from equation (6). We will assume that $h_{0,0}$ converges; $h_{0,0}$ characterizes the intrinsic strength of the coalescence interaction, independently of any particular collision rate or number size distribution.

[20] We shall see that at least in the power law domain of attraction (i.e., those initial conditions which evolve toward power law distributions), the main quantitative aspect of H which is important is given by $h_{0,0}$. The subscripts "0,0" are used because $h_{0,0}$ is simply one of a hierarchy of coefficients defined by H; the other members of the hierarchy turn out only to be important for the stability properties; see Appendix B.

[21] To determine the conditions on $H(V, V')$ necessary for the convergence of $h_{0,0}$, and following *Van Dongen and Ernst* [1987], we introduce a large λ exponent ω such that

$$H(1,\lambda) \approx \lambda^{\beta-\omega}; \qquad \lambda \gg 1 \tag{8}$$

[22] Since for large λ the bracketed term in equation (7) is of order unity when $\beta < 1$, we see that $h_{0,0}$ converges when $\omega > 0$ (if $\beta > 1$, then convergence requires $\omega > \beta - 1$); such convergence corresponds to *Van Dongen and Ernst*'s [1987] "class 1" kernel. If in addition, $\omega > \beta$, then the interactions are primarily among bubbles with similar volumes hence the large bubbles are mostly the result of a hierarchical series of coalescence of smaller nearly equisized bubbles: the coalescence process has a cascade phenomenology as described in *Gaonac'h et al.* [1996b].

[23] It suffices for our results that $\boldsymbol{H}$ satisfies the fairly general properties. However, for concreteness, we note that still under fairly general conditions $\boldsymbol{H}$ is of the following form:

$$\boldsymbol{H}(\boldsymbol{V}, \boldsymbol{V}', t) = E(\boldsymbol{V}, \boldsymbol{V}')\left(\boldsymbol{V}^{1/3} + \boldsymbol{V}'^{1/3}\right)^2 \boldsymbol{\Delta u}(\boldsymbol{V}, \boldsymbol{V}', t) \tag{9}$$

where $\Delta\boldsymbol{u}(\boldsymbol{V}, \boldsymbol{V}', t)$ is the absolute velocity difference (shear) between bubbles of size $\boldsymbol{V}$, and $\boldsymbol{V}'$ and E is the dimensionless efficiency factor: it is homogeneous of order $\beta = 0$ (see equation (5a)); that is, it depends only on the volume ratios $\lambda = \boldsymbol{V}'/\boldsymbol{V}$. The interpretation of equation (9) is straightforward; the middle term is the geometric cross section for collisions, and the collision rate depends on the velocity differences between the two bubbles. In a volcanic conduit, this velocity difference will arise primarily because of shearing: both because the overall flow rate is highest near the center of the conduit but also locally due to the expansion of bubbles as they rise.

[24] The efficiency factor E is the fraction of collisions that result in coalescence. As discussed by *Manga and Stone* [1994], since small bubbles tend to flow around large bubbles, $E(\lambda)$ does indeed fall off, for large and small volume ratio λ. Although the value of ω is not known empirically, it is almost certainly >0 (implying convergence of $h_{0,0}$) and could indeed be $>\beta$ ($\approx$0.85 [*Gaonac'h et al.*, 1996a, 2004]) as required for a cascade phenomenology. Although viscosity may influence the efficiency its effect will primarily be on the shear term. For example, if we assume that the bubbles follow the magma field (as, for example, in Plinian eruptions), then $\Delta\boldsymbol{u}$ is proportional to the stress, inversely proportional to the local viscosity. The possible temporal variation of the latter will determine φ.

[25] To be even more explicit in our interpretation, it may be useful to consider the expression $\Delta\boldsymbol{u}(\boldsymbol{V}, \boldsymbol{V}', t)$ used in meteorology and introduced into volcanology by *Sahagian* [1985] (here representing the absolute difference in bubble velocities):

$$\boldsymbol{u}(\boldsymbol{V}, t) = \boldsymbol{u}_0(t)\boldsymbol{V}^{\gamma} \tag{10}$$

$$\begin{aligned} \boldsymbol{\Delta u}(\boldsymbol{V}, \boldsymbol{V}', t) &= \phi(t)|\boldsymbol{V}^{\gamma} - \boldsymbol{V}'^{\gamma}| \\ \phi(t) &= \boldsymbol{u}_0(t)\boldsymbol{V}_0^{2/3} \end{aligned} \tag{11}$$

where $\boldsymbol{u}_0(t)$ is the (generally time varying) velocity of the bubble of volume $\boldsymbol{V}_0$ and $\gamma = \beta - 2/3$ is the fundamental velocity exponent. As mentioned by *Gaonac'h et al.* [1996b], in low Reynolds number flows if we assume the bubble velocities are purely due to buoyancy forces, then we obtain $\gamma = 2/3$ from dimensional analysis. However, this is presumably not relevant in magmas where buoyancy-induced shears are unlikely to be important in comparison with dynamically imposed shears (i.e., externally forced). Specific models such as this would give a more precise physical interpretation of φ; for example $\boldsymbol{u}_0(t)\boldsymbol{V}_0^{2/3}$ is the mean volume swept out per unit time by bubbles of volume $\boldsymbol{V}_0$.

3. Solutions

3.1. Vesicularity

[26] The first step in the solution of the dimensionless expansion-coalescence equation (4) is to obtain an equation for the vesicularity. Defining the latter by

$$P(t) = \int_0^{\infty} Vn(V,t)dV \tag{12}$$

we can immediately obtain the equation for the evolution of P by multiplying the expansion-coalescence equation (4) by VdV and integrating over all V. This shows that the coalescence terms do not change the vesicularity (this can be seen by straightforward manipulations [see, e.g., *Drake*, 1972]; hence we obtain

$$\frac{dP}{dt} = P\xi(t) \tag{13}$$

Equation (13) is just a restatement of the fact that in the expansion-coalescence equation, the vesicularity is entirely determined by the decompressive expansion effect (whatever its origins): on its own, coalescence conserves the vesicularity. Solving this equation, we obtain:

$$\frac{P(\tau)}{P(0)} = F(\tau) = \exp\left[\int_0^{\tau} \xi(\tau')d\tau'\right] = \exp\left[\int_0^{t} \xi(t')dt'\right] \tag{14}$$

where F is the intrinsically dimensionless total (time integrated) decompressive expansion factor since the beginning of the expansion. Note that physically, $P(t) \leq 1$; in addition the equations will no longer be valid when P approaches the percolation threshold where ternary and

higher-order bubble interactions become important (for $B = 0.85$, this is near 70%; see *Gaonac'h et al.* [2003]). Equation (14) establishes a one-to-one relation between the nondimensional time τ and the vesicularity; in principle it can be inverted: all the solutions developed below can therefore be expressed purely in terms of P, not τ.

3.2. Scaling Solutions

[27] A basic mathematical property of the coalescence equation known since the 1970s is that if $B = \beta$, then the pure scaling function

$$n(V,\tau) = n_0(\tau)V^{-1-B} \tag{15}$$

is a solution of equation (4); $n_0(\tau)$, which contains all the time varying information, is the "amplitude" of the number density $n(V,\tau)$. In this case, we find by substitution of $n(V,\tau)$ from equation (15) into equation (4) that $n_0(\tau)^{-1}$, is a solution of the first-order, ordinary linear differential equation

$$\frac{dn_0^{-1}}{d\tau} + B\xi n_0^{-1} = h_{0,0} \tag{16}$$

where $h_{0,0}$ is the coalescence interaction coefficient (equation (7)). Since the term in the parentheses in equation (7) is >0 for $\beta < 1$ and <0 for $\beta > 1$, we find $h_{0,0} > 0$ for $\beta < 1$; and $h_{0,0} < 0$ for $\beta > 1$; the fact that $h_{0,0} > 0$ for $\beta < 1$ indicates that for $\xi = 0$ (pure coalescence) $n_0(t)$ decreases under the action of coalescence whereas for $\beta > 1$ $n_0(t)$ increases.

[28] As it stands, this exact solution is of purely academic interest, since in general, pure power law number densities are physically unacceptable because of various divergences (infinities) that they imply. Various truncations/cutoffs are necessary in order for them to be useful physical models. The full details for any value of B are given by *Gaonac'h et al.* [1996a], here for brevity, we only consider the cases $0 < B < 1$, $B > 1$.

[29] 1. When $0 < B < 1$ (the range apparently empirically relevant for magma), the total number of bubbles per volume $\int n(V)dV$ diverges due to the small V behavior. This is generally not physically important and can be avoided if necessary by the introduction of a small volume cutoff in the distribution so that the power law only holds for larger V. What is more serious is that the total vesicularity $\int Vn(V)dV$ also diverges because of the large V behavior. This is physically unacceptable and requires a large V truncation/cutoff at V^*. The bubbles with volumes near V^* thus give the dominant contribution to the total vesicularity (full details are given below).

[30] 2. When $B > 1$, the total number density still diverges due to the small V behavior; however, now the vesicularity also diverges due to this small V behavior so that a small V cutoff is absolutely necessary. In contrast, at large V there is no longer any problem, the large bubbles are simply too rare to give a significant contribution to the total vesicularity. This is the range of B which is apparently relevant for multibody coalescence ("percolation" [see *Gaonac'h et al.*, 2003]) and for posteruption volcanic product fragments [see *Kaminski and Jaupart*, 1998].

3.3. Similarity Solutions With a Cutoff $V^*(t)$

[31] We are now in a position to present the central results of the paper. We have mentioned that the problem with the pure power law solution (equation (15)) is that for $B < 1$, the vesicularity diverges; we therefore need to introduce a cutoff at large V. The simplest way to do this is to generalize slightly the similarity method of *Friedlander* [1961], i.e., to introduce the following ansatz (functional form):

$$n(V,\tau) = n_0(\tau)V^{-1-B}f(z)$$
$$z = \frac{V}{V^*(\tau)} \tag{17}$$

where f is a cutoff function and $V^*(\tau)$ is the volume cutoff (for a given f, V^* will determine the vesicularity; see below). As the overall vesicularity increases because of compressive expansion, V^*, which is essentially the largest bubble in the system, will evolve as will the amplitude $n_0(\tau)$; they are both required to determine the vesicularity.

[32] We can now use the result of *Van Dongen and Ernst* [1987], who show that the leading large V behavior is exponential; this suggests the following:

$$f(z) = e^{-z}g(z) \tag{18}$$

where $g(z)$ is expected to be slowly varying (subexponential). Substituting this ansatz into the coalescence-expansion equation (4) and using relation (23a) below between P and V^* to eliminate $\partial z/\partial\tau$, we obtain

$$\left(\frac{dn_0^{-1}}{d\tau} + B\xi n_0^{-1}\right)\left(g(z)\left(1 - \frac{z}{1-B}\right) + \frac{z}{1-B}g'(z)\right)$$
$$= \int_0^\infty e^{-z\lambda}g(z)g(\lambda z)\lambda^{-1-B}H(1,\lambda)d\lambda$$
$$- \int_1^\infty g\left(\frac{z}{1+\lambda}\right)g\left(\frac{z\lambda}{1+\lambda}\right)\left(\frac{1+\lambda}{\lambda}\right)^B H(1,\lambda)\lambda^{-1}d\lambda \tag{19}$$

Dividing both sides by the second term in parentheses on the left, we find that the left-hand side is only a function of time, while the right-hand side is only a function of z; hence using standard separation of variables arguments, they must each be equal to a constant. Without loss of generality, we can choose the constant as $h_{0,0}$ so that the equation for $n_0(t)$ is the same as that without the truncation:

$$\frac{dn_0^{-1}}{d\tau} + B\xi n_0^{-1} = h_{0,0} \tag{20}$$

while $g(z)$ satisfies

$$h_{0,0}\left[g(z)\left(1 - \frac{z}{1-B}\right) + \frac{z}{1-B}g'(z)\right]$$
$$= \int_0^\infty e^{z\lambda}g(z)g(\lambda z)\lambda^{-1-B}H(1,\lambda)d\lambda - \int_1^\infty g\left(\frac{z}{1+\lambda}\right)g\left(\frac{z\lambda}{1+\lambda}\right)$$
$$\cdot \left(\frac{1+\lambda}{\lambda}\right)^B H(1,\lambda)\lambda^{-1}d\lambda \tag{21}$$

We can now verify by substituting $z = 0$, that $g(0) = 1$. For the large z behavior, substitution of the ansatz $g \approx z^{\alpha}$ shows that for any scaling H exponent $\beta = B$, we obtain $\alpha = 1$, i.e., g is asymptotically linear; we conclude

$$g(z) \approx \begin{matrix} 1; & z \approx 0 \\ z & z \gg 1 \end{matrix} \tag{22}$$

so that $g(z)$ is indeed slowly varying (subexponential; i.e., negligible with respect to an exponential) as required. If H is known, equation (21) can be solved numerically for g; however, the exact solution will only lead to small (second-order) changes in the $n(V, t)$; the first-order effect only depends on the interaction kernel H via $h_{0,0}$.

[33] In order to determine V^* (parameterized by τ or t) we use the vesicularity relation, equation (14) with $f(z) = e^{-z}g(z)$:

$$\begin{aligned} P(\tau) &= p_B \frac{n_0(\tau)V^*(\tau)^{1-B}}{1-B} \\ p_B &= (1-B)\int_0^{\infty} e^{-z}z^{-B}g(z)dz \end{aligned} \tag{23a}$$

The constant p_B depends only on H and B; the factor $1 - B$ in the definition is chosen since for all g, it gives

$$p_B \approx O(1) \tag{23b}$$

[34] For example, in the case of a step-function-type cutoff function: $g(z) = 1$, $z < 1$, $g(z) = 0$, $z > 1$, it gives $p_B = 1$, whereas for $g(z) = 1$ it gives $p_B = (1 - B)\Gamma(1 - B)$; which implies $0.8856 < p_B < 1$ for $0 < B < 1$. Since $g(z)$ is slowly varying with $g(0) = 1$, we therefore expect p_B to be close to 1; p_B can also be estimated empirically as described below.

[35] The solution for the first-order, linear ordinary differential equation for the reciprocal of the amplitude of the number density n_0^{-1} (equation (20)) is straightforward (using for example the method of integrating factors); we obtain

$$\begin{aligned} n_0^{-1}(\tau) &= \left(\frac{P(\tau)}{P(0)}\right)^{-B} n_0^{-1}(0) + h(\tau) \\ h(\tau) &= h_{0,0}P^{-B}(\tau)\int_0^{\tau} P^B(\tau')d\tau' \end{aligned} \tag{24}$$

where $h(\tau)$ is the particular solution; τ' is a dummy variable, physically $h(\tau)$ represents the total coalescence interaction of the volcanic bubbles up to time τ, Figure 4 shows a schematic. Appendix B now shows that the solutions are stable and attractive implying that initial distributions which are not truncated power laws will, nevertheless, tend to evolve toward such solutions, as long as they are within the power law domain of attraction; i.e., this can remain true even in the presence of diffusion and other perturbing processes.

3.4. Summary of the Key Results

[36] Starting from an initial truncated power law solution, equations (17), (18), (23a), and (24) are the solutions for the entire system; for any scaling interaction kernel, any coalescence-expansion history. Perhaps the simplest way to display the solution is to parameterize the process using the porosity. In this case these key equations can be written as

$$\begin{aligned} h(P) &= h_{0,0}P^{-B}\int_{P_0}^{P} \frac{P'^B dP'}{(dP'/d\tau')} = h_{0,0}P^{-B}\int_{P_0}^{P} P'^{B-1}\frac{dP'}{\xi(P')} \\ n_0(P) &= \frac{n_0(P_0)P_0^{-B}}{P^{-B} + P_0^{-B}h(P)} \\ V^*(P) &= \left(\frac{(1-B)P}{p_B}\right)^{1/(1-B)} n_0(P_0)^{-1/(1-B)} \approx \left(\frac{(1-B)P}{n_0(P_0)}\right)^{1/(1-B)} \\ n(V,P) &= n_0(P)V^{-1-B}e^{-V/V^*}g\left(\frac{V}{V^*}\right) \approx n_0(P)V^{-1-B}e^{-V/V^*} \end{aligned} \tag{25}$$

where $P_0 = P(0)$ is the initial vesicularity. In order to use equations (25) to determine the number density of the vesicles, as a preliminary, we must first start with the interaction kernel H and calculate the interaction coefficient $h_{0,0}$. For mathematically exact solutions, we must also plug H into equation (21) and then solve it for g; from g we calculate p_B (equation (23a)). In actual fact, we expect to obtain excellent approximations with $p_B = g = 1$ (hence the approximate equalities on the far right of equation (25)). This preliminary step just depends on the type of interaction; H. For the next step, we require information about the particular magma history: more precisely, we need the vesicularity history $P(\tau)$ which relates the porosity and (nondimensional) time. From this, we calculate the total interaction $h(P)$ (top line of equation (25), it is obtained from equation (24) writing the integral for h in terms of $P(\tau)$ rather than $\tau(P)$; since τ is empirically inaccessible, it may be more practical to use the relation $d\tau = dP/(P\xi)$ obtained from equation (13)). We can then compute the number density amplitude $n_0(P)$ (second line, it is also obtained from equation (24)). Finally, we calculate the cutoff V^* which is the largest vesicle volume. It can be determined by inverting equation (23a) (more precisely, V^* is the characteristic exponential volume cutoff; there will be a few slightly larger vesicles). The actual number density is finally given by using the above values of $n_0(P)$, V^* in equation (17) with $f(V/V^*) = e^{-(V/V^*)}$ and g either = 1 (the approximation) or g is the solution of equation (19) as indicated above. Appendix C gives a number of analytic examples.

[37] A few comments are in order. First, $h(\tau)$ represents the total coalescence interaction over the entire duration of the expansion/coalescence process. With pure decompressive expansion, $h_{0,0} = 0$, and $h(\tau) = 0$ while for pure coalescence, $h(\tau) = h_{0,0}$. From equation (24), we see that the relative importance of $h(\tau)$ with respect to $[P(\tau)/P(0)]^{-B}n_0^{-1}$ (0) determines the importance of coalescence with respect to pure decompressive expansion. Assuming a constant decompressive expansion rate ξ_0, we already obtain the simple solution of equation (24):

$$n_0^{-1}(P) = n_0^{-1}(P_0)\left(\frac{P}{P_0}\right)^{-B} + \frac{h_{0,0}}{B\xi_0}\left(1 - \left(\frac{P}{P_0}\right)^{-B}\right) \tag{26}$$

So that for large enough expansion ratios P/P_0, the distribution achieves an asymptotic state independent of the initial $n_0(P_0)$: $n_0(\tau) \approx (B\xi_0/h_{0,0})$. A useful general result illustrated by the models in Appendix C is that since

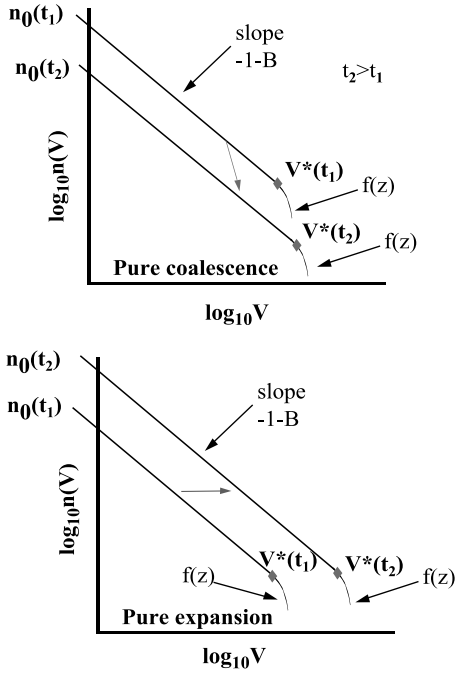

Figure 4. (top) Effect of pure coalescence when $B < 1$, $h_{0,0} > 1$ so that n_0 decreases in time. On a log-log plot the distributions shift downward, while the cutoff (V^*) increases. (bottom) Effect of pure decompressive expansion. All bubbles increase in size by the same factor, and the distribution is shifted to the right. See color version of this figure in the HTML.

in $h(\tau)$, $(P(\tau')/P(\tau))^B < 1$ we therefore have $h(\tau) < \tau h_{0,0}$ and for many models/scenarios, $h(\tau) \approx \tau h_{0,0}$. Although they are of somewhat academic interest, various simplified (analytically tractable) models are discussed in Appendix C.

3.5. Coalescence Enhancement of the Large Bubbles

[38] The main effect of the coalescence is to attract the distribution of bubbles to the truncated power law form; this will occur even if the total interaction between these bubbles $h(\tau)$ is not so large. However, when $h(\tau)$ becomes important, coalescence can also greatly enhance the size of the large bubbles with respect to the small ones. Using equations (23a) and (24) we can obtain a formula for the "enhancement," i.e., the factor G above and beyond the effect of pure decompressive expansion:

$$G = \left(\frac{V^*(P)}{V^*(P_0)}\right) / \left(\frac{P}{P_0}\right) = \left[1 + \frac{(1-B)}{p_B} P_0 \left(\frac{P}{P_0}\right)^B h\right]^{1/(1-B)} \tag{27}$$

Equation (27) shows that there are two coalescence regimes. When the interaction is small enough, i.e., when

$$\frac{(1-B)}{p_B} P_0 \left(\frac{P}{P_0}\right)^B h < 1 \tag{28}$$

then $G(1) \approx 1$ and coalescence can be ignored. If we assume that the final vesicularity $P \approx 1$ and since $B \approx 1$, $P_0^{1-B} \approx 1$, $p_B \approx 1$, we obtain $(1 - B)h < 1$. In the case of constant decompressive expansion rate, we further obtain $h \approx h_{0,0}/B\xi_0$ so that the weak coalescence condition reduces to

$$h_{0,0} < \frac{B\xi_0}{(1-B)} \tag{29}$$

When the interaction is weak enough or the expansion rate strong enough, coalescence is unimportant (see, however, some of the singular examples in Appendix C).

[39] Conversely, when the interaction coefficient between bubbles $h_{0,0}$ is large enough, coalescence can give a large enhancement of the size of the large bubbles. Under the same assumptions on p_B, h, P we obtain

$$G \approx \frac{P_0}{P} \left(\frac{(1-B)h_{0,0}}{B\xi_0}\right)^{1/(1-B)}; G > 1 \tag{30}$$

Even if the interaction coefficient is not very large, we may still conclude that the main effect of coalescence is to establish the stable power law form. In any case, it is an important empirical task to estimate $h_{0,0}$. As an illustration of the type of behavior that we might expect, we can use the particular kernel of equation (9) (with Δu given by equation (11)) and assuming a pure power law $E(\lambda) = \lambda^{-\omega}$ ($\lambda > 1$). Figure 5 shows the result, indicating that $h_{0,0} < 1$ for all $\omega > 0.46$ (diverging, however, as $\omega \to 0$).

3.6. Empirical Tests

[40] The nondimensional solutions we have obtained for the amplitude of the distribution $\boldsymbol{n}_0(\tau)$ are not always the most convenient. In practice it is sometimes more convenient (see below) to define a new (dimensional) density amplitude factor $\boldsymbol{n}_0^*(\tau)$:

$$\boldsymbol{n}_0^*(\tau) = \boldsymbol{n}(\boldsymbol{V}^*, \tau) \frac{e}{g(1)} \tag{31}$$

so that the basic solution (equation (17)) can be written

$$\boldsymbol{n}(\boldsymbol{V}, \tau) = \boldsymbol{n}_0^*(\tau) \left(\frac{\boldsymbol{V}}{\boldsymbol{V}^*(\tau)}\right)^{-1-B} e^{-\boldsymbol{V}/\boldsymbol{V}^*(\tau)} g\left(\frac{\boldsymbol{V}}{\boldsymbol{V}^*(\tau)}\right) \tag{32}$$

[41] This leads to

$$\boldsymbol{n}_0^* \boldsymbol{V}^{*2} = \frac{(1-B)}{p_B} P = \boldsymbol{n}_0 \boldsymbol{V}^{*(1-B)} \tag{33}$$

or

$$\boldsymbol{n}_0 = \boldsymbol{n}_0^* \boldsymbol{V}^{*(1+B)} \tag{34}$$

the couple ($\boldsymbol{n}^*$, $\boldsymbol{V}^*$) provides a convenient characterization of the distribution since it is determined directly by the truncation point on a log-log plot of $\boldsymbol{n}$ (Figure 4). Using equations (27) and (14), we have

$$\boldsymbol{n}_0^*(\tau) = G(\tau)^{-2} F(\tau)^{-1} \boldsymbol{n}_0^*(0) \tag{35}$$

Although the theory can be tested without knowing the actual time elapsed, only the vesicularity P and large bubble growth factors F (pure decompressive expansion) and G

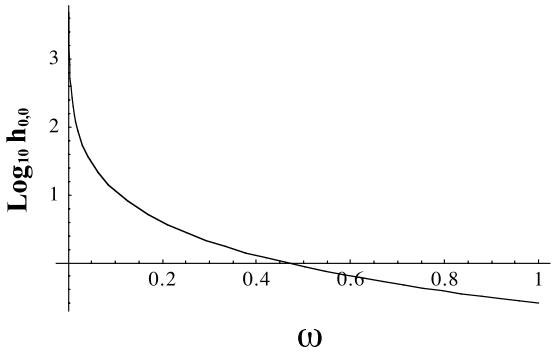

Figure 5. Interaction coefficient $h_{0,0}$ as a function of the exponent ω of the collision efficiency (estimated using the geometric cross section as discussed in section 2, equations (9) and (11)). A large ω indicates interactions are inefficient unless the bubbles have nearly the same size (see the definition equation (8)).

(coalescence enhancement) are needed, this information may still be difficult to obtain since the only easily accessible bubble distribution information is from solidified samples. This explains why for the moment, the main empirical test of the theory is the near power law distributions observed in both lava and pumice as demonstrated in Figure 2 [see also *Gaonac'h et al.*, 1996a, 2004]. However, even at a single time further information may be obtainable; it may be possible to empirically confirm the near exponential nature of the large $\boldsymbol{V}$ cutoff: according to equation (31), we expect $\log(\boldsymbol{n}(\boldsymbol{V})\boldsymbol{V}^{1+B})$ to be linear with $\boldsymbol{V}$ which could be used to estimate $\boldsymbol{V}^*$, and hence $g(1)$, $\boldsymbol{n}_0^*$ from equations (31) and (32). We could also empirically estimate $\boldsymbol{p}_B$ by estimating $P(\tau)$ and using equation (23). Unfortunately, the key dynamical parameters ω (characterizes the interaction between bubbles of very different sizes, equation (8)), $h_{0,0}$ (the interaction coefficient, equation (7)), $h(\tau)$ (the total coalescence interaction up to time τ, equation (24)), are not directly accessible from single samples at a single time.

[42] If identical bubbling melts could be frozen after different degrees of decompression in controlled laboratory experiments, then this would furnish the information (e.g., *Simakin et al.*, 1999). Alternatively, we may be able to use statistics on measured $\boldsymbol{V}^*$, $\boldsymbol{n}^*$ parameters. At present, the only possibility is to follow the approach of *Herd and Pinkerton* [1997] who argue that in volcanic bombs, the change in the bubble size distribution from the center to the edge of the bomb is primarily governed by the cooling process that is fastest near the surface. The expansion-coalescence process therefore has more time to act near the central region than near the periphery; by comparing the distributions near the center and edge we might therefore be able to test the theory and estimate the function $h(P)$.

[43] To illustrate the idea, in Figure 6 we replot the distributions from *Herd and Pinkerton*'s [1997, Figure 8] sample RH/S9. Although the data are noisy (the sample size was inevitably not large), we see that the theoretical power law behavior is reasonably followed for the large bubbles. The rapid rate of bubble falloff of the large edge bubbles is as roughly predicted by the exponential truncation theory, although it may be influenced by large bubbles directly degassing to the atmosphere. In addition, the physical properties change rapidly near the edge and the actual distribution measured is thus somewhat of a mixture of bubbles, which were "frozen in" at slightly different times (rather than at the same time as assumed for the purposes of this analysis). We now consider that the distribution at different distances from the center represents identically evolving distributions arrested at various τ. We have from equations (33) and (35):

$$\frac{\boldsymbol{n}^*_{0,\text{edge}}}{\boldsymbol{n}_{0,\text{center}^*}} = \frac{G(\text{center})^2 F(\text{center})}{G(\text{edge})^2 F(\text{edge})}$$
$$\frac{\boldsymbol{V}^*_{\text{edge}}}{\boldsymbol{V}^*_{\text{center}}} = \frac{G(\text{edge})F(\text{edge})}{G(\text{center})F(\text{center})} \tag{36}$$

From the graph, we find $\boldsymbol{n}_{0\ \text{center}}{}^*/\boldsymbol{n}_{0\ \text{edge}}{}^* = 10^{-0.8}$, and $\boldsymbol{V}_{\text{center}}{}^*/\boldsymbol{V}_{\text{edge}}{}^* = 10^{0.6}$; hence $P(\text{center})/P(\text{edge}) = F(\text{center})/F(\text{edge}) = 10^{0.4}$ and $G(\text{center})/G(\text{edge}) = 10^{0.2}$. The estimate of $F(\text{center})/F(\text{edge})$, which is roughly equal to the vesicularity ratio estimated by *Herd and Pinkerton* [1997] (0.60/0.25 = 2.4). Clearly, this method could be applied to intermediate distances between the center and the edge thus yielding the function $G(F)$ which could then be analyzed.

[44] If a cooling curve for the sample could be established, then the distance from the edge of the sample would give us the relative times. By systematically comparing the number distributions as functions of distance from the edge, we could then estimate $(\boldsymbol{n}_0{}^*(\tau), \boldsymbol{V}^*(\tau))$ as well as $P(\tau)$. We could then directly exploit equation (20) in the form

$$P^{-B}(\tau)\frac{d\left(P^B(\tau)n_0^{-1}(\tau)\right)}{d\tau} = h(\tau) \tag{37}$$

for small enough time intervals, the derivative could be numerically estimated and hence $h(\tau)$ could be determined. Similarly, the expansion rate could be estimated by

$$\xi(\tau) = \frac{d(\log P)}{d\tau} \tag{38}$$

from the vesicularity values. Once P, ξ and the collision rate φ are known, then $h(\tau)$ could be determined. Clearly, large data sets would have to be analyzed to establish if the assumptions of this method are really valid and to improve the statistical significance of the result.

4. Conclusions

[45] Magma rising from depth exsolves gas first by nucleation, diffusion, and decompressive expansion, eventually obtaining high vesicularities prior to fragmentation and explosion. As the bubbles grow, single bubble processes such as diffusion become increasingly less efficient whereas coalescence becomes more efficient; the expanding, rising bubbles induce shearing in the magma, and shearing induces coalescence; it is difficult to avoid the conclusion that binary coalescence plays a dominant role – at least for the larger bubbles at the higher vesicularities. At high enough vesicularities, binary coalescence itself becomes dominated by ternary and higher-order interactions until, as discussed by *Gaonac'h et al.* [2003], a critical percolation threshold is

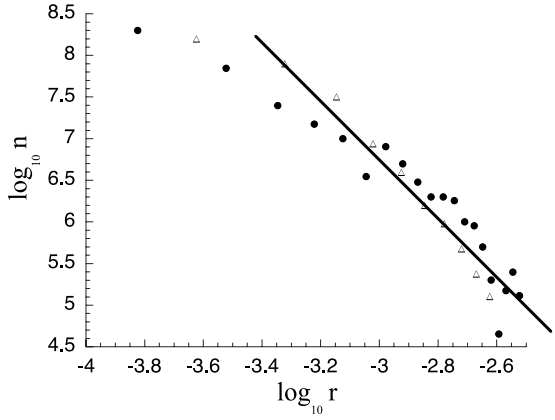

Figure 6. Replot of distributions from *Herd and Pinkerton* [1997, Figures 8a and 8c] for the "edge" (triangles) and "center" (circles). The edge distribution has been multiplied by $10^{-0.8}$ (a downward shift of 0.8 corresponding to $\boldsymbol{n}_{0\ \mathrm{center}}^{*}/\boldsymbol{n}_{0\ \mathrm{edge}}^{*} = 10^{-0.8}$), and a rightward shift of $10^{0.2}$ (corresponding to $\boldsymbol{V}_{\mathrm{center}}^{*}/\boldsymbol{V}_{\mathrm{edge}}^{*} = 10^{0.6}$, i.e., the ratio of the large bubble volumes). Note that using $\boldsymbol{n}_0^*$ rather than $\boldsymbol{n}_0$ is a bit easier since we attempt to superpose the entire curves rather than just the small $\boldsymbol{r}$ part. The straight line has the theoretical slope $-(3B + 1) = -3.55$. Units are $\boldsymbol{r}$ in m and $\boldsymbol{n}$ in $\mathrm{m}^{-3}(\mathrm{mm}^{-1})$.

reached where the magma essentially fragments due to an infinite network of tentacle-like overlapping bubbles. Binary coalescence plays a fundamental role since the exponent it apparently establishes [*Gaonac'h et al.*, 2004] allows the magma to avoid percolation until realistic values of 70% are achieved. The observed scaling of the bubble distribution turns out to provide exactly the necessary "packing" efficiencies.

[46] We argued that to a good approximation, over a wide range of vesicularities and conditions (e.g., pumice and lavas), that bubble dynamics can be reasonably modeled by the decompression and coalescence of an initial distribution of small bubbles using the (binary) expansion-coalescence equation. A typical scenario would be the decompression of rising magma followed by exsolution of gas around nucleation centers. As the magma continues to rise, these small bubbles expand. At some critical but small gas concentration level, coalescence starts to dominate the diffusion and surface tension effects, first for the large bubbles, then later for all but the smallest. Eventually, near the percolation threshold, multibody coalescence takes over, but binary coalescence has already played a key role primarily in establishing a power law bubble distribution, and also in enhancing the size of the largest bubbles. Our theory applies to the expansion- coalescence dominated regime; we considered first pure expansion-coalescence, and then consider surface tension and diffusion as additional small perturbations. The strongest support for the model is the growing empirical evidence in favor of power law number densities.

[47] The basic physical assumption is that the collision/interaction kernel is scaling so that over a wide range, the fundamental interaction mechanism depends only on the ratios of the volumes of the interacting bubbles. This assumption is almost universally made in the coalescence literature and can be at least partially justified on the basis of fluid mechanical considerations. The key result is that exact truncated power law solutions are possible for any expansion rate history ($\xi(t)$). By systematically exploiting these stable attractive solutions, we reduce the problem from a nonlinear integropartial differential equation into a simple initial value problem: a first-order linear ordinary differential equation for the inverse bubble density amplitude $\boldsymbol{n}_0(t)^{-1}$.

[48] By considering several eruption scenarios (including eruption events as singularities in the relative expansion-collision rates) it was found that as long as the bulk of the expansion occurred early in the overall coalescence process, that the result (determined by the collision integral $h(\tau)$) was quite insensitive to the details.

[49] Although the cutoff power law solutions are mathematically exact, they would be physically irrelevant if they were unstable. In Appendix B we therefore performed linear stability analysis and derived the conditions under which the power law solutions are stable to small perturbations. We also showed how to take into account diffusion and surface tension effects as small perturbations: they both will increase the instability of the singular ($q > 0$) perturbations, i.e., lead to breaks in the scaling at small volumes, as observed. A remarkable aspect of the problem is that most of the details of the coalescence interaction kernel are irrelevant; it is primarily the interaction coefficient $h_{0,0}$ and the scaling exponent B, which are important. The other details of the coalescence kernel ($h_{q,q'}$ in Appendix B) simply determine the stability of the scaling solutions to perturbations.

[50] So far, the empirical support for this theory has come almost exclusively from the basic scaling symmetry apparently respected by bubble size distributions in pumice and lavas. Beyond this, it is not obvious how to test the theory; to do so would require knowledge about the temporal evolution of the bubble size distribution. We suggest a possible method based on the work of *Herd and Pinkerton* [1997], which uses volcanic bombs. The idea is that because of differential cooling of the bomb after eruption/ejection the outside and inside have different bubble distributions due to the longer time available for coalescence near the center. By reanalyzing some of their data we show how this can be used to obtain information about the fundamental interaction integral. Unfortunately, information about the fundamental interaction coefficient $h_{0,0}$ will probably require laboratory experiments involving binary bubble events.

[51] Although it is generally recognized that coalescence processes are important in the evolution of bubble populations in magma, the theoretical treatment of the (linear) single bubble growth processes has been so much easier that attention has often been focused on the corresponding diffusion and surface tension mechanisms. However, in this paper, the simplifications introduced promise to make the study of coalescence much easier. Indeed, this reduction coupled with the agreement between the power law behavior predicted by the expansion-coalescence equation and the empirical vesicle distributions found in a wide variety of lava and pumice samples, make this approach quite seductive. However, it should be recalled that use of a slightly different scaling symmetry by *Gaonac'h et al.*

[2003] led to similar power law distributions but implicitly involved ternary and higher-order interactions. Much more work, including laboratory studies of bubble interactions, will be therefore be needed.

Appendix A: Single Bubble Processes: Expansion, Diffusion, and Surface Tension

[52] In most bubble growth processes (expansion, diffusion, surface tension) we can neglect direct bubble-bubble interactions and consider the bubbles in isolation. In this appendix, we consider such single bubble processes and show how they modify the (two bubble) coalescence equation.

[53] In single bubble processes, the rate of change in volume w depends only on the volume and time:

$$\frac{dV}{dt} = w(V,t) \tag{A1}$$

[54] As concerns equation (1) (the partial differential equation for $\partial n/\partial t$), these single bubble processes contribute the terms:

$$-\frac{\partial(nw)}{\partial V} \tag{A2}$$

[55] The single bubble processes of interest are of the form

$$w(V,t) = \mu(t)V^{\delta} \tag{A3}$$

for diffusion we have $\delta = 1/3$, $\mu > 0$, and Ostwald ripening, $\delta = 0$, $\mu > 0$, surface tension, $\delta = 2/3$, $\mu < 0$. (Strictly speaking, Ostwald ripening is a multibubble process; however, the usual "mean field" treatment allows it to be treated as an "effectively" single bubble process with the rate given above.) Note that even if $w(V, t)$ is a power law function of volume (and considering only single body processes), the evolving number density will be a power law in V only if very special initial conditions and/or constraints are imposed. For example, it is usually assumed that diffusion gives rise to an exponential $n(V, t)$, but *Blower et al.* [2001] argue that special hierarchically organized (i.e., scaling) constraints could enable diffusion to produce a power law $n(V, t)$.

[56] The main case of interest here is the case of expansion ($\delta = 1$); we introduce the (generally) time varying expansion coefficient ($\xi(t)$, i.e., $w(V, t) = V\xi(t)$) which determines how individual bubbles size V will expand in time:

$$\frac{dV}{dt} = \xi(t)V \tag{A4}$$

($\xi > 0$ corresponds to expansion). Mathematically, expansion is particularly simple since the term it contributes is "equidimensional" (here, this means invariant if the bubble volumes are replaced by volumes λ times larger, see equation (A2)).

[57] Specializing to the expansion case of primary interest here, we obtain the expansion-coalescence equation (4). Equation (4) has been considered in the context of cloud drop growth by *Srivastava and Passarelli* [1980] (who showed how it could be reduced, by transformation of variables, to a pure coalescence problem). Generalizations to arbitrary power law growth laws have been considered in the polymer physics literature [*Cueille and Sire*, 1997].

Appendix B: Stability of the Power Law Solutions

B1. Linear Stability

[58] The coalescence-expansion equations are nonlinear; hence there is the possibility that the exact solutions discussed above may be unstable and hence be physically irrelevant. *Van Dongen and Ernst* [1987] use scaling arguments on the pure coalescence equation to argue that for a wide variety of initial conditions, at large times the cutoff power law will be obtained. To our knowledge, however, direct investigation of the stability using linear stability theory has not been performed. In this appendix we consider the linear stability of the pure power law solution of the coalescence-expansion equation. To simplify the equations and to simultaneously emphasize the quadratic nonlinearity with respect to n, we introduce the following quantum mechanical like "bra" and "ket" notation:

$$\begin{aligned}\langle n(V,\tau)|H|n(V,\tau)\rangle = -\frac{1}{2}\int_0^V H(V-V',V') \\ \cdot n(V-V',t)n(V',\tau)dV' \\ + n(V,\tau)\int_0^{\infty} H(V,V')n(V',\tau)dV'\end{aligned} \tag{B1a}$$

which indicates the operator H acting on the function n; the resulting dimensionless expansion coalescence equation can now be written

$$\frac{\partial n(V,\tau)}{\partial \tau} = -\xi(\tau)\frac{\partial(n(V,\tau))}{\partial V} - \langle n(V,\tau)|H|n(V,\tau)\rangle \tag{B1b}$$

This makes the writing much more compact while emphasizing the quadratic nonlinearity with respect to n.

[59] Continuing to simplify notation, we introduce the normalized density:

$$\mathsf{N}(V,\tau) = V^{B+1}n(V,\tau) \tag{B2a}$$

which satisfies

$$\frac{\partial \mathsf{N}(V,\tau)}{\partial \tau} = -\xi(\tau)V^{\mathsf{B}+1}\frac{\partial\left(V^{-\mathsf{B}}\mathsf{N}\right)}{\partial V} - \langle \mathsf{N}|\mathsf{H}|\mathsf{N}\rangle \tag{B2b}$$

with the normalized kernel H defined by

$$\langle a|\mathsf{H}|b\rangle = V^{B+1}\left\langle aV^{-B-1}|\mathsf{H}|bV^{-B-1}\right\rangle \tag{B3}$$

for any functions $a(V, \tau)$, $b(V, \tau)$. Finally, define the V-independent generalized interaction coefficient $h_{q,q'}$:

$$\left\langle V^{-q}|\mathsf{H}|V^{-q'}\right\rangle = V^{-q-q'}h_{q,q'} \tag{B4}$$

Note that the pure power law solution $n(V, \tau) = n_0(\tau)V^{-1-B}$ corresponds to $N(V, \tau) = n_0(\tau)$. Introduce $N'(V, \tau)$ which is the perturbation around the pure power law solution:

$$\mathsf{N}(V,\tau) = n_0(\tau) + \mathsf{N}'(V,\tau) \tag{B5}$$

substituting this into equation (B2) and identifying the V-dependent and V-independent terms, we obtain the unperturbed equation

$$\frac{dn_0^{-1}}{d\tau} + B\xi n_0^{-1} = h_{0,0} \tag{B6a}$$

for $n_0(\tau)$, yielding the solution

$$n_0^{-1}(\tau) = n_0^{-1}(0)F^{-B}(\tau) + h(\tau) \tag{B6b}$$

($F(\tau) = P(\tau)/P(0)$) and the following equation for the perturbation:

$$\frac{\partial \mathsf{N}'(V,\tau)}{\partial \tau} = -\xi(\tau)V^{B+1}\frac{\partial\left(V^{-B}\mathsf{N}'\right)}{\partial V} - n_0(\tau) \cdot \left[\langle 1|\mathsf{H}|\mathsf{N}'\rangle + \langle \mathsf{N}'|\mathsf{H}|1\rangle\right] - \langle \mathsf{N}'|\mathsf{H}|\mathsf{N}'\rangle \tag{B7}$$

The linear perturbation equation is obtained by neglecting the quadratic term $\langle N'|H|N'\rangle$. Since homogeneous kernels have simple behaviors for power law distributions, it is convenient to introduce the Mellin transform and its inverse:

$$\begin{aligned} \overline{\mathsf{N}'}(q,\tau) &= \int_0^\infty \mathsf{N}'(V,\tau)V^{q-1}dV \\ \mathsf{N}'(V,\tau) &= \frac{1}{2\pi i}\int_{-i\infty+\varepsilon}^{i\infty+\varepsilon} \overline{\mathsf{N}'}(q,\tau)V^{-q}dq \end{aligned} \tag{B8}$$

where ε is any real constant which allows the integrals to converge. Substituting this into the above and in the nonlinear term we therefore obtain

$$\left[\frac{\partial}{\partial\tau} - \xi(\tau)(q+B) + n_0(\tau)\left(h_{0,q} + h_{q,0}\right)\right] \cdot \overline{\mathsf{N}}'(q,\tau) = -\frac{1}{2\pi i}\overline{\mathsf{N}}'(q,\tau)\int_{-i\infty+\varepsilon}^{i\infty+\varepsilon} h_{q,q'}\overline{\mathsf{N}'}(q',\tau)dq' \tag{B9}$$

Neglecting the right-hand quadratic term and introducing the relative perturbation $w_q(\tau)$:

$$w_q(\tau) = \frac{\overline{\mathsf{N}'}(q,\tau)}{n_0(\tau)} \tag{B10}$$

we obtain the linear perturbation equation for $w_q(\tau)$:

$$\frac{\partial \log w_q}{\partial\tau} = q\xi(\tau) + n_0(\tau)\left(h_{0,0} - h_{0,q} - h_{q,0}\right) \tag{B11}$$

If the amplitude of the relative perturbation decreases in time, then the perturbation is stable, i.e., if for all time,

$$\frac{\partial \log|w_q|}{\partial\tau} < 0 \tag{B12}$$

Since $\log|w_q| = \mathrm{Re}(\log w_q)$, the condition for stability is

$$\mathrm{Re}\left(q\xi(\tau) + n_0(\tau)\left(h_{0,0} - h_{0,q} - h_{q,0}\right)\right) < 0 \tag{B13a}$$

with $n_0(\tau)$ given by equation (B6b) and with $\mathrm{Re}(q) = \varepsilon$ fixed but allowing for any value of $y = \mathrm{Im}(q)$ (this is because the Mellin transform involves the integral along a line parallel to the imaginary axis). It is not hard to show from the definition of $h_{q,q'}$ that

$$\max_y\left[\mathrm{Re}\left(h_{0,\varepsilon+iy} + h_{\varepsilon+iy,0}\right)\right] = h_{0,\varepsilon} + h_{\varepsilon,0}$$

so that a necessary and sufficient condition for the decrease of $w_q = |\overline{N'}(q,\tau)/n_0(\tau)|$ is that

$$\begin{aligned} \varepsilon\xi(\tau) + n_0(\tau)\left(h_{0,0} - h_{0,\varepsilon} - h_{\varepsilon,0}\right) < 0 \\ \varepsilon = \mathrm{Re}(q) \end{aligned} \tag{B13b}$$

Finally, we use the following inequality

$$h_{0,0} < \left(h_{0,\varepsilon} + h_{\varepsilon,0}\right); \varepsilon < (1-B)/2 \tag{B14}$$

to conclude that for $B < 1$, that $\varepsilon < 0$ is a sufficient condition for stability is that $w_q = |\overline{\mathsf{N}'}(q,\tau)/n_0(\tau)|$ decreases (since, assuming expansion, i.e., $\xi > 0$, both terms in equation (B13) will be <0). More precisely, depending on the exact values of ξ, $n_0(\tau)$, there will be a critical value ε_{cr} with $0 < \varepsilon_{cr} < (1 - B)/2$; all perturbations in N of the form V^{-q} (perturbations in n of the form V^{-1-B-q}) will be stable for $\mathrm{Re}(q) < \varepsilon_{cr}$. When $\mathrm{Re}(q) < 0$, the perturbations correspond to regularities in V (dominated by large V), when $\mathrm{Re}(q) > 0$, they correspond to singularities (dominated by small V).

[60] To summarize, our stability analysis has shown that under expansion ($\xi > 0$) all perturbations $n_q'(V,\tau) = \overline{\mathsf{N}'}(q,\tau)V^{-q-B-1}$, with systematic excess of large bubbles ($\mathrm{Re}(q) < 0$) with respect to unperturbed solution $n_0(\tau)V^{-1-B}$ will be stable; indeed, stability continues up to $0 < \mathrm{Re}(q) = \varepsilon_{cr} < (1 - B)/2$. For $\mathrm{Re}(q) > \varepsilon_{cr} > 0$ stability is no longer guaranteed. These perturbations will grow at least initially (they could be stabilized by the nonlinear term, or by other physics) and will correspond to deviations from pure V^{-1-B} behavior primarily for small enough V.

B2. Large Volume Cutoff as a Perturbation

[61] Since the similarity (scaling) solution with the exponential cutoff is an exact solution, which does indeed approach a pure power law as $\tau \to \infty$ (as $V^*(\tau) \to \infty$), it is clear that the domain of attraction of the pure power law is quite large. It is quite straightforward to show that the basin of attraction extends to drastic (step function) cutoffs.

[62] To show that an initial distribution with such a drastic cutoff does indeed approach a pure power law at large τ, note that such a cutoff distribution can be represented as a pure power law with the following perturbation:

$$\begin{aligned} \mathsf{N}'(V,\tau=0) &= -n_0(0); V > V^*(0) \\ \mathsf{N}'(V,\tau=0) &= 0; V < V^*(0) \end{aligned} \tag{B15}$$

[63] Therefore, performing the Mellin transform, we obtain

$$\begin{aligned} \overline{\mathsf{N}'}(q,0) = \int_0^\infty \mathsf{N}'(V,0)V^{q-1}dV &= \frac{n_0(0)}{q}V^{*q}; \quad \mathrm{Re}\, q < 0 \\ &= -\infty; \quad \mathrm{Re}\, q > 0 \end{aligned} \tag{B16}$$

[64] The perturbation is small if the ratio

$$\frac{\overline{\mathsf{N}'}(q,0)}{n_0(0)} = \frac{V^{*_q}}{q} \ll 1 \tag{B17}$$

this smallness criterion can be satisfied for any $V^* > 1$ by taking $\mathrm{Re}(q) = \varepsilon < 0$ sufficiently negative. We conclude that the above perturbation theory is applicable with perturbations having $\varepsilon < 0$; hence the drastic cutoff is in the power law domain of attraction, and solutions will be asymptotically pure power laws.

B3. Diffusion and Surface Tension

[65] The presence of diffusion adds a term: $-\mu(\tau)\partial(V^{\delta}n)/\partial V$ (with $\mu(\tau) > 0$ for growth, $\delta = 1/3$ "parabolic" growth law, $\delta = 0$, Ostwald ripening, $\mu(\tau) > 0$ is the rate) to the basic equation while surface tension adds a corresponding term with $\delta = 2/3$ (but with $\mu < 0$). If the absolute rate $\mu(\tau)$ is small, we can treat such effects as perturbations. To see this, consider the equation for the normalized density $N(V, \tau)$ but with a diffusion/surface tension term added:

$$\frac{\partial \mathsf{N}(V,\tau)}{\partial \tau} = -\xi(\tau)V^{B+1}\frac{\partial(V^{-B}\mathsf{N})}{\partial V} - \langle \mathsf{N}|\mathsf{H}|\mathsf{N}\rangle - \mu(\tau)V^{B+1} \cdot \frac{\partial\left(V^{\delta-B-1}\mathsf{N}\right)}{\partial V} \tag{B18}$$

If we now take $\mathsf{N}(V, \tau) = n_0(\tau)\mathsf{N}'(V, \tau)$ and assume that $n_0(\tau)$ is the power law solution of the unperturbed equation (B6a), then we obtain

$$\begin{aligned}\frac{\partial \mathsf{N}'(V,t)}{\partial \tau} = &-\xi(\tau)V^{B+1}\frac{\partial\left(V^{-B}\mathsf{N}'\right)}{\partial V} - n_0(\tau)\left[\langle 1|\mathsf{H}|\mathsf{N}'\rangle + \langle \mathsf{N}'|\mathsf{H}|1\rangle\right] \\ &- n_0(\tau)\mu(\tau)V^{B+1}\frac{\partial\left(V^{\delta-B-1}\right)}{\partial V} - \mu(\tau)V^{B+1}\frac{\partial\left(V^{\delta-B-1}\mathsf{N}'\right)}{\partial V} \\ &- \langle \mathsf{N}'|\mathsf{H}|\mathsf{N}'\rangle\end{aligned} \tag{B19}$$

Since μ is taken to be small, for linear perturbation we may neglect the last two terms which will be second order in small quantities. The remaining diffusion/surface tension term

$$n_0(\tau)\mu(\tau)(1 + B - \delta)V^{\delta-1} \tag{B20}$$

will only affect the $q = -\delta + 1$ Mellin coefficient $\overline{\mathsf{N}'}(1 - \delta, \tau)$; so these effects add an inhomogeneous term to equation (B9). Ignoring the second-order terms this becomes

$$\begin{aligned}\frac{\partial \log w_q}{\partial \tau} = &\xi(\tau)(1-\delta) + n_0(\tau)\left(h_{0,0} - h_{0,1-\delta} - h_{1-\delta,0}\right) \\ &+ w_q^{-1}\mu(\tau)(1 - \delta + B)\end{aligned} \tag{B21}$$

Even without the new (far right) term, we can see that the above is unstable for any $1 - \delta > \varepsilon_{cr}$ i.e., for any $\delta < (1 + B)/2$ and that the new term with $\mu(\tau) > 0$ (diffusion) makes it more unstable while $\mu < 0$ (surface tension, $\delta = 2/3$), will be more stable. Taking $B = 0.8$, we see $\varepsilon_{cr} = 0.1$, so that terms with $\delta < 0.9$ (which include the surface tension and diffusion effects) will indeed lead to increased instability of the power law, and since these correspond to $q > \varepsilon_{cr} > 0$, these effects will be most important at small V; indeed, *Gaonac'h et al.* [1996a, 2004] show that for small V the power behavior does indeed break down.

Appendix C: Some Empirical and Analytic Eruption Models

[66] In order to better understand the expansion-coalescence processes it is useful to consider analytic solutions, even if these may seem a little academic. In this appendix, we examine several.

[67] Recalling $F(\tau) = P(\tau)/P(0)$ and using the identity

$$F^{-B}\frac{d\left(F^B n_0^{-1}\right)}{d\tau} = \frac{dn_0^{-1}}{d\tau} + B\tilde{\xi}n_0^{-1}$$

equation (19) may be rewritten

$$\frac{d\left(F^B n_0^{-1}\right)}{d\tau} = F^B h(\tau) \tag{C1a}$$

Since $F(0) = 1$, this implies that

$$n_0^{-1}(\tau) = F^{-B}(\tau)n_0^{-1}(0) + h(\tau) \tag{C1b}$$

where $n_0(0)$ is the initial n_0 at the beginning of the process and the interaction strength $h(\tau)$ is

$$h(\tau) = h_{0,0}\int_0^{\tau}\left(\frac{F(\tau')}{F(\tau)}\right)^B d\tau' \tag{C1c}$$

Since τ simply parameterizes the evolution and the entire process is of finite duration, for convenience in the rest of this appendix, we will take $\tau = 0$ at the beginning of the process and $\tau = 1$ at the end. Since in the above integral $F(\tau')/F(\tau) < 1$, we see that the total interaction strength at the end of the expansion-coalescence process $h(\tau = 1)$ is bounded above by $h_{0,0}$ for any non contracting process ($\xi > 0$). This is easy to see since the expanding process which gives the largest $h(\tau)$ clearly is

$$\begin{aligned}\xi(\tau) &= \xi_0\delta(\tau) \\ F(\tau) &= e^{\xi_0};\tau > 0 \\ h(\tau) &= h_{0,0};\tau > 0\end{aligned} \tag{C2}$$

In addition, for reasonable physical models, we expect $h(1) \approx h_{0,0}$ as we show below via examples.

[68] The expansion-coalescence process begins in the magma chamber when gas-laden magma rises to a level where exsolution can begin, i.e., where the pressure is low enough for the magma to be supersaturated and where the nucleation rate is sufficiently high. We can now consider several simple expansion-coalescence models and their corresponding interaction functions $h(\tau)$.

C1. Pure Coalescence

[69] When $\xi(\tau) = 0$, we obtain pure coalescence, $F(\tau) = P(0) = 1$ and

$$h(\tau) = h_{0,0}\tau \tag{C3}$$

$$n_0^{-1}(\tau) = n_0^{-1}(0) + h_{0,0}\tau \tag{C4}$$

So that $h(1) = h_{0,0}$ (the theoretical maximum).

C2. Constant Expansion Rates

[70] In this case we may take

$$\xi(\tau) = \xi_0 = \text{const}$$
$$n_0^{-1}(\tau) = n_0^{-1}(0) + h_{0,0}\tau \tag{C5}$$

this yields

$$F(\tau) = e^{\xi_0 \tau}$$
$$h(\tau) = \frac{h_{0,0}}{B\xi_0}\left(1 - e^{-\xi_0\tau}\right) = \frac{h_{0,0}}{B\xi_0}\left(1 - F^{-B}\right) \tag{C6}$$

Note that for large total expansion ($F \gg 1$), $h(1) \approx h_{0,0}/B$. This yields

$$n_0^{-1}(F) = n_0^{-1}(F=1)F^{-B} + \frac{jh_{0,0}}{B\xi_0}\left(1 - F^{-B}\right) \tag{C7}$$

where we have written $n_0(F(\tau))$ with the initial $n_0 = n_0(F = 1)$. This shows that for large F, $n_0(F)$ asymptotes to the value $B\xi_0/h_{0,0}$. The actual time elapsed (including the detailed changes in collision rate and expansion rate) is thus irrelevant; it is only the total expansion (F) that matters.

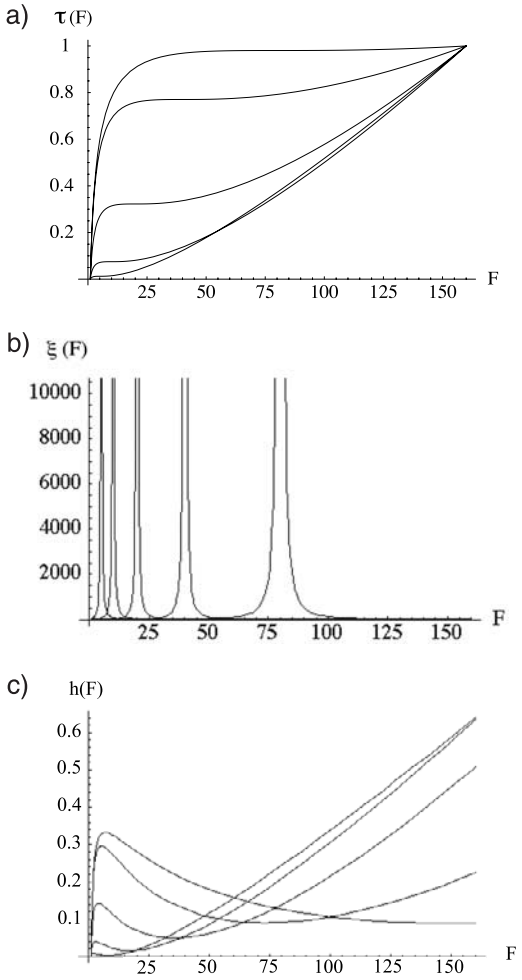

Figure C1. (a) Plot of $\tau(F)$ for $F(1) = 160$, with $F_0 = 5$, 10, 20, 40, 80 (top to bottom), $H = 0.5$. (b) Plot of $\xi(F)$ for $F(1) = 160$, with $F_0 = 5$, 10, 20, 40, 80 (left to right), $H = 0.5$. (c) Plot of $h(F)$ for $h_{0,0} = 1$ and $F(1) = 160$, with $F_0 = 5$, 10, 20, 40, 80 (top to bottom on right).

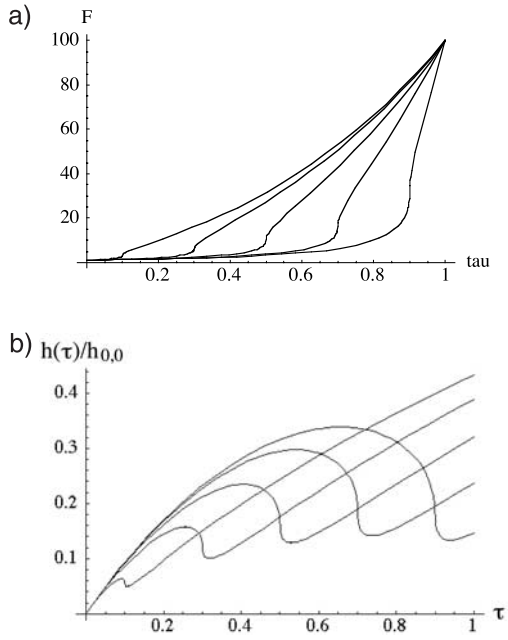

Figure C2. (a) Singular model with $F(1) = 100$, for $\tau_0 = 0.1, 0.3, 0.5, 0.7, 0.9$. (b) Corresponding interaction integral for $F(1) = 100$, for $\tau_0 = 0.1, 0.3, 0.5, 0.7, 0.9$.

C3. Singular Eruption Models

[71] The above two examples show a general feature: that we may parameterize the process by the vesicularity ratio F rather than τ, indeed from equation (14) we see that

$$\left(F\frac{d\tau}{dF}\right)^{-1} = \xi(\tau) \tag{C8}$$

$$h(F) = h_{0,0}F^B \int_1^F F'^B \left(\frac{d\tau}{dF'}\right) dF' = h_{0,0}F^B \int_1^F F'^{B-1}\frac{dF'}{\xi} \tag{C9}$$

We can use this to generate some rather general models in the following way. Consider a single term in a (generalized) power expansion for the normalized expansion rate ξ:

$$\xi = AF^\alpha \tag{C10}$$

this implies

$$\tau = -\frac{F^{-\alpha}}{A\alpha}$$
$$h(F) = \frac{h_{0,0}(F^{-\alpha} - F^{-B})}{A(B-\alpha)} \tag{C11}$$

Similar simple results hold for log terms. We can now use linear combinations of such terms to create a singular model for an eruption event. For example,

$$\xi = \frac{a}{\left(F^H - F_0^H\right)^2} \tag{C12}$$

This represents a second-order singularity at $F = F_0$ (the exponent H is added for somewhat greater flexibility but it doesn't change the order of singularity at F_0). The parameter A is a normalization constant which determines the total overall expansion factor. This singular model yields

$$\tau(F) = \frac{2}{aH}F_0^H\left(1-F^H\right) - \frac{1}{2aH}\left(1-F^{2H}\right) + \frac{F_0^{2H}}{a}\log F$$
$$h(F) = \frac{h_{0,0}}{a}\left(\frac{(F^{2H}-F^{-B})}{B+2H} - \frac{2F_0^H(F^H-F^{-B})}{B+H} + \frac{F_0^H(1-F^{-B})}{B}\right) \quad \text{(C13)}$$

Figures C1a, C1b, and C1c show the typical evolution of $\tau(F)$, $\xi(F)$, and $h(F)/h_{0,0}$ for various model parameters. If it is specified that the total expansion factor is $F(1)$, then a is determined by the condition $\tau(F(1)) = 1$.

[72] From equation (C12) (and Figure C1a) we see that the smaller F_0, the sooner the bulk of the expansion occurs; that is, the eruption occurs for smaller τ. Figure C1c indicates that the earlier the eruption the larger the overall effect of the coalescence $h(\tau)$ (for small F_0, it is close to its theoretical maximum ($=h_{0,0} = 1$ in Figure C1c).

C4. Other Singular Models

[73] Continuing with the idea of representing an eruptive event as a singularity, we can use the following model with singularity order 1/2 (with respect to τ, not F) at $\tau = \tau_0$:

$$\xi(\tau) = \left(\frac{|\tau_0-\tau|^{-1/2}}{2\sqrt{\tau_0}+2\sqrt{1-\tau_0}}\right)\log F(1) \quad \text{(C14)}$$

$$\log F(\tau) = \int_0^\tau \xi(\tau')d\tau' = \begin{cases}\left(\frac{\sqrt{\tau_0}-\sqrt{\tau_0-\tau}}{\sqrt{\tau_0}+\sqrt{1-\tau_0}}\right)\log F(1); \tau < \tau_0 \\ \left(\frac{\sqrt{\tau_0}+\sqrt{\tau-\tau_0}}{\sqrt{\tau_0}+\sqrt{1-\tau_0}}\right)\log F(1); \tau > \tau_0\end{cases} \quad \text{(C15)}$$

(the order 1/2 was chosen because the integrals for ξ, h are both analytic). Figures C2a and C2b show the corresponding $F(\tau)$, $h(\tau)$ functions for a fixed total expansion factor (=100) and with the eruption event occurring at different relative fractions of the overall coalescence process. Once again, as long as the eruption is fairly early on we find $h(\tau = 1) \approx h_{0,0}$.

[74] **Acknowledgment.** We acknowledge several very useful discussions with Claude Jaupart and critical comments by Sylvie Vergniolle and an anonymous referee.

References

Blower, J. D., J. P. Keating, H. M. Mader, and J. C. Phillips (2001), Inferring volcanic degassing processes from vesicle size distributions, *Geophys. Res. Lett.*, *28*, 347–350.

Brown, P. S. (1995), Structural stability of the coalescence/breakup equation, *J. Atmos. Sci.*, *52*, 3857–3865.

Cueille, S., and C. Sire (1997), Smoluchowski's equation for cluster exogeneous growth, *Europhys. Lett.*, *40*, 239–244.

Drake, R. L. (1972), A general mathematical survey of the coagulation equation, in *Topics in Current Aerosol Research 3*, vol. II, edited by G. M. Hidy and J. R. Brock, pp. 201–376, Pergamon, New York.

Friedlander, S. K. (1961), Theoretical considerations for the particle size spectrum of the stratospheric aerosol, *J. Meteorol.*, *18*, 753–759.

Gaonac'h, G., J. Stix, S. Lovejoy, and D. Schertzer (1996a), Scaling effects on vesicle shape, size and heterogeneity of lavas from Mount Etna, *J. Volcanol. Geotherm. Res.*, *74*, 131–153.

Gaonac'h, G., J. Stix, S. Lovejoy, and D. Schertzer (1996b), A scaling cascade model for bubble growth in lavas, *Earth Planet. Sci. Lett.*, *139*, 395–409.

Gaonac'h, H., S. Lovejoy, and D. Schertzer (2003), Percolating magmas and explosive volcanism, *Geophys. Res. Lett.*, *30*(11), 1559, doi:10.1029/2002GL016022.

Gaonac'h, G., S. Lovejoy, and D. Schertzer (2004), Scaling vesicle distributions and volcanic eruptions, *Bull. Volcanol.*, doi:10.1007/500445-004-0376-4.

Gardner, J. E., R. M. E. Thomas, C. Jaupart, and S. Tait (1996), Fragmentation of magma during Plinian volcanic eruptions, *Bull. Volcanol.*, *58*, 144–162.

Herd, R. A., and H. Pinkerton (1997), Bubble coalescence in basaltic lava: Its impact on the evolution of bubble populations, *J. Volcanol. Geotherm. Res.*, *75*, 137–157.

Kaminski, E., and C. Jaupart (1998), The size distribution of pyroclasts and the fragmentation sequence in explosive volcanic eruptions, *J. Geophys. Res.*, *103*, 29,759–29,779.

Klug, C., K. V. Cashman, and C. R. Bacon (2002), Structure and physical characteristics of pumice from the climactic eruption of Mount Mazama (Crater Lake), Oregon, *Bull. Volcanol.*, *64*, 486–501.

Lee, M. H. (2000), On the validity of the coagulation equation and the nature of runaway growth, *Icarus*, *143*, 74–86.

Lushnikov, A. A. (1972), Evolution of coagulating systems, *J. Colloid Interface Sci.*, *45*, 549–556.

Manga, M., and H. A. Stone (1994), Interactions between bubbles in magmas and lavas: Effects of bubble deformation, *J. Volcanol. Geotherm. Res.*, *63*, 267–279.

Mangan, M., and T. Sisson (2000), Delayed, disequilibrium degassing in rhyolite magma: Decompression experiments and implications for explosive volcanism, *Earth Planet. Sci. Lett.*, *183*, 441–455.

Meunier, J. L., and R. Peschanski (1992), Intermittency, fragmentation and the Smoluchowski equation, *Nucl. Phys. B*, *374*, 327–339.

Sahagian, D. L. (1985), Bubble migration and coalescence during the solidification of basaltic flows, *J. Geol.*, *93*, 205–211.

Simakin, A. G., P. Armienti, and M. B. Epel'baum (1999), Coupled degassing and crystallization: Experimental study at continuous pressure drop, with application to volcanic bombs, *Bull. Volcanol.*, *61*, 275–287.

Smoluchowski, M. V. (1916), Versuch einer mathematischen Theorie des Koagulationskinetic kolloider Lösunger, *Z. Phys. Chem.*, *92*, 129–168.

Sparks, R. S. J. (1978), The dynamics of bubble formation and growth in magmas, *J. Volcanol. Geotherm. Res.*, *3*, 1–37.

Srivastava, R. C., and R. E. Passarelli (1980), Analytical solutions to simple models of condensation and coalescence, *J. Atmos. Sci.*, *37*, 612–621.

Turco, R. P., and F. Yu (1999), Particle size distributions in an expanding plume undergoing simultaneous coagulation and condensation, *J. Geophys. Res.*, *104*, 19,227–19,241.

Van Dongen, P. G. J. (1987), Solution of Smoluchowski's coagulation equation at large cluster sizes, *Physica A*, *145*, 15–66.

Van Dongen, P. G. J., and M. H. Ernst (1987), Tail distribution of large clusters form the coagulation equation, *J. Colloid Interface Sci.*, *115*, 27–35.

Van Dongen, P. G. J., and M. H. Ernst (1988), Scaling solutions of Smoluchowski's coagulation equation, *J. Stat. Phys.*, *50*, 295–329.

H. Gaonac'h, GEOTOP, UQAM, Succ. Centre-Ville, Montréal, Quebec, Canada H3C 3P8. (gaonach.helene@uqam.ca)

S. Lovejoy, Department of Physics, McGill University, 3600 University St., Montréal, Quebec, Canada H3A 2T8. (lovejoy@physics.mcgill.ca)

D. Schertzer, CEREVE, Ecole Nationale des Ponts et Chaussées, 6-8, avenue Blaise Pascal, Cité Descartes, F-77455 Marne-la-Vallée Cedex, France. (daniel.schertzer@cereve.enpc.fr)